

## 1/f noise in $\delta$ -doped GaAs analyzed in terms of mobility fluctuations

X. Y. Chen, P. M. Koenraad, F. N. Hooge, and J. H. Wolter

*COBRA, Interuniversity Research Institute, Department of Electrical Engineering and Department of Physics, Eindhoven University of Technology, 5600 MB Eindhoven, The Netherlands*

V. Aninkevicius

*Semiconductor Physics Institute, A. Gostauto 11, 2600 Vilnius, Lithuania*

(Received 28 June 1996; revised manuscript received 3 October 1996)

This paper presents  $1/f$  noise measurements on Si  $\delta$ -doped GaAs structures. The samples are characterized by Hall, magnetoresistance, and Schubnikov–de Haas measurements. The distribution of electrons over the two lowest subbands in these structures varies with temperature and illumination, and so does the noise. The  $1/f$  noise is characterized by the usual parameter  $\alpha$ . We show in detail how to interpret the  $1/f$  noise in the two-subbands system. We find that  $\alpha$  increases by a factor of 30 upon population of a second subband either by illuminating the sample or by raising the temperature to 100 K. This strong increase in the  $1/f$  noise is successfully described by the mobility fluctuation model, where only the lattice scattering contributes to the  $1/f$  noise. The  $1/f$  noise of the electrons in both subbands can be characterized by the same value of  $\alpha_L=0.4$ , which is strong support for the model. [S0163-1829(97)00308-1]

### I. INTRODUCTION

Many semiconductor devices suffer from  $1/f$  noise. Before anything can be done to remedy this, we need to understand the physical nature of this type of noise. The study of the origin of  $1/f$  noise requires simple well-defined samples: a  $\delta$ -doped layer is such a structure.

The ideas about  $1/f$  noise in semiconductors are moving toward a model of mobility fluctuations in the bulk of the material. Yet, there still is experimental evidence that in some cases  $1/f$  noise might be generated by traps at the surface which would mean that  $1/f$  noise is a fluctuation in the number of electrons (e.g., metal-oxide-semiconductor transistor).

The Eindhoven group proposed a model in which the mobility fluctuations are due to the lattice scattering only.<sup>1,2</sup> The strongest experimental evidence they presented for their point of view is from the noise of a series of similar devices where the impurity scattering varies because of different doping levels. ‘‘Diluting’’ the constant lattice scattering with noise-free impurity scattering reduces the  $1/f$  noise systematically. Although the acceptance of the mobility model is growing, the problem is far from settled. Therefore, we undertook this noise study of  $\delta$ -doped layers in order to find different experimental arguments for the model.

In the first place the conducting  $\delta$ -doped layer is far from the surface and there are no interfaces such as those found in two-dimensional heterostructures. Second, the electrons in the  $\delta$ -doped layer are distributed over different subbands, each with its own mobility and contribution to the noise. The important point is that the electrons in different subbands are scattered by the same lattice vibrations in the same volume. The model then predicts the same contribution from lattice scattering to the  $1/f$  noise.

Typically, a  $\delta$ -doped layer of Si in GaAs, grown at a low temperature, has a thickness of only a few atomic layers. Due to the narrow size of the potential well of a  $\delta$ -doping layer, a

two-dimensional electron gas (2DEG) is formed at the doping plane. Because the doping concentration is above the Mott density ( $\approx 3 \times 10^{11} \text{ cm}^{-2}$  for GaAs:Si), there is no carrier freeze out at low temperatures. A typical picture of the electronic band structure of the  $\delta$ -doped layer is shown in Fig. 1. The electrons may populate several subbands in the potential well. The scattering cross section of electrons on the ionized donor atoms is different for electrons in different subbands, because the electron wave functions have different  $z$  dependences. The electron mobility in each subband depends, in a complicated way, on the shape of the wave func-

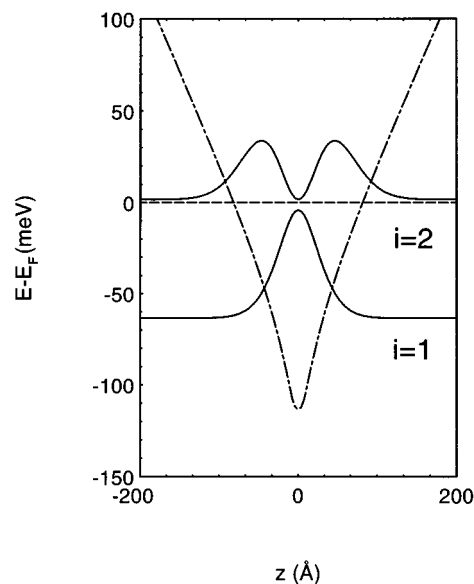


FIG. 1. The electronic structure of a  $\delta$ -doped layer. The dashed-dotted line represents the potential well. The dashed line presents the Fermi level. The solid lines represent the subband levels and the electron wave functions. The second subband is a few meV above the Fermi level.

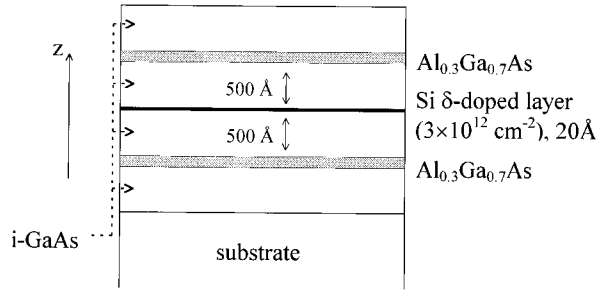


FIG. 2. Cross-section of the sample.

tion, the population of the level, and the screening. Experimental and theoretical analysis have shown that the mobility in a higher subband is higher than in a lower subband.<sup>3</sup>

The electronic properties of  $\delta$ -doped layers have been studied intensively. Compared with homogeneously doped GaAs, significant advantages in the electronic properties have been found in  $\delta$ -doped structures.<sup>4</sup> Some different devices have been developed by using  $\delta$ -doped layers.<sup>5,6</sup> In this contribution, the results of noise measurements on a  $\delta$ -doped structure are presented.

We carried out measurements in the temperature range of 77 to 300 K. We experimentally changed the distribution of the electrons over the subbands either by illuminating the sample with a red light-emitting diode or by increasing the temperature above 100 K. We studied the influence of this redistribution on the  $1/f$  noise. The results enable us to demonstrate that the  $1/f$  noise is due to mobility fluctuations related to phonon scattering exclusively.

## II. SAMPLE GROWTH AND CHARACTERIZATION

### A. Sample growth

The sample was grown in our Varian-Gen II molecular-beam epitaxy. The structure consists of a Si  $\delta$ -doped layer centered between two  $\text{Al}_{0.3}\text{Ga}_{0.7}\text{As}$  barriers each at 500 Å away from the  $\delta$ -doped layer. We used a low growth temperature of 480 °C to limit the thickness of the doping layer to 20 Å.<sup>7</sup> This part of the structure is grown on top of a 1  $\mu\text{m}$ -thick GaAs buffer layer. A schematic diagram showing the layer structure is given in Fig. 2. The  $\delta$ -doping layer

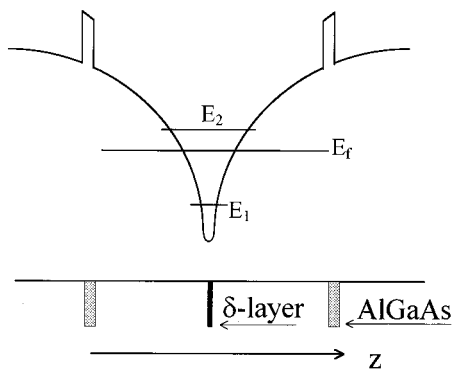


FIG. 3. Schematic diagram of the structure of the conduction band of the sample. 1 and 2 indicate subbands 1 and 2.  $E_f$  is the Fermi level.

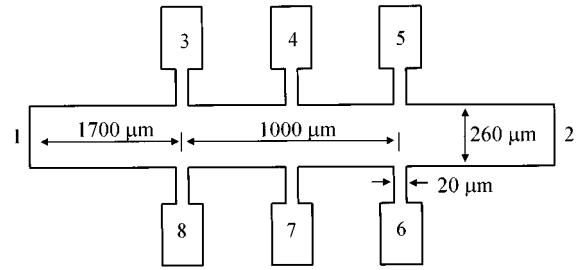


FIG. 4. Geometry of the sample. The numbers 1–8 refer to contacts; 1 and 2 are used as current contacts.

contained about  $3 \times 10^{12}$  Si atoms per  $\text{cm}^2$ . In our GaAs structures grown at 480 °C we typically find a  $p$ -type background concentration of about  $10^{15} \text{ cm}^{-3}$ , this is about a factor 10 higher than in GaAs grown at the optimal growth temperature of 650 °C. The  $p$ -type background concentration in  $\text{Al}_{0.3}\text{Ga}_{0.7}\text{As}$  grown at this low temperature proved to be much higher than  $10^{15} \text{ cm}^{-3}$ . We find values in the range of  $10^{17}$ – $10^{18} \text{ cm}^{-3}$ . A schematic diagram of the conduction band in the structure is shown in Fig. 3. A Hall bar structure was prepared by the conventional lithography process. Ohmic contacts were made by annealing Sn balls on the surface of the sample at 450 °C in an atmosphere of  $\text{N}_2/\text{H}_2$ . The configuration of the sample is given in Fig. 4.

### B. Hall characterization

The samples were first characterized by simple Hall measurements. We prepared the samples into either Van der Pauw structures or Hall bar structures as given in Fig. 4. The samples are characterized as a function of temperature from 5 up to 300 K. We characterized the samples in the dark and

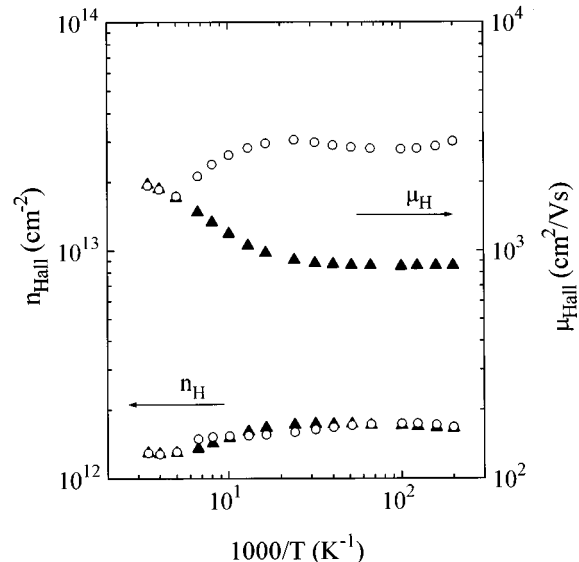


FIG. 5. Temperature dependencies of the surface Hall concentration and Hall mobility. The solid symbols represent the results in the dark, and the open symbols present the results after illumination.

TABLE I. Characteristics of the sample. SdH: Schubnikov–de Haas measurement from which the quantum mobility is obtained. CMR: Classical magnetoresistance measurement from which the transport mobility is obtained. Hall: Hall measurement. PPC (5 K): Persistent photoconductance (PPC) after illumination at 5 K. PPC (77 K): PPC after illumination at 77 K.

|       |           | $n_H$ ( $10^{12}$ cm $^{-2}$ ) | $\mu_H$ ( $10^3$ cm $^2$ /V s) | $n_1$ ( $10^{12}$ cm $^{-2}$ ) | $n_2$ ( $10^{12}$ cm $^{-2}$ ) | $\mu_1$ (cm $^2$ /V s) | $\mu_2$ (cm $^2$ /V s) |                |
|-------|-----------|--------------------------------|--------------------------------|--------------------------------|--------------------------------|------------------------|------------------------|----------------|
| 5 K   | Dark      | SdH                            |                                | $1.88 \pm 0.02$                | 0                              | $460 \pm 30$           |                        |                |
|       |           | CMR                            |                                | $1.91 \pm 0.02$                | 0                              | $950 \pm 50$           |                        |                |
|       | PPC (5 K) | Hall                           | $1.60 \pm 0.03$                | $900 \pm 50$                   |                                |                        |                        |                |
|       |           | SdH                            |                                |                                | $2.11 \pm 0.02$                | $0.50 \pm 0.02$        | $600 \pm 80$           | $2150 \pm 150$ |
|       |           | CMR                            |                                |                                | $2.0 \pm 0.1$                  | $0.4 \pm 0.1$          | $1400 \pm 100$         | $4100 \pm 200$ |
|       |           | Hall                           | $1.68 \pm 0.03$                | $2900 \pm 100$                 |                                |                        |                        |                |
| 77 K  | Dark      | CMR                            |                                | $1.70 \pm 0.02$                | 0                              | $1050 \pm 50$          |                        |                |
|       |           | Hall                           | $1.58 \pm 0.03$                | $900 \pm 50$                   |                                |                        |                        |                |
|       | PPC (5 K) | CMR                            |                                |                                | $2.0 \pm 0.1$                  | $0.24 \pm 0.03$        | $1400 \pm 50$          | $5200 \pm 300$ |
|       |           | Hall                           | $1.58 \pm 0.03$                | $2900 \pm 100$                 |                                |                        |                        |                |
|       |           | CMR                            |                                |                                | $1.88 \pm 0.03$                | $0.17 \pm 0.02$        | $1220 \pm 30$          | $3900 \pm 100$ |
|       |           | Hall                           | $1.62 \pm 0.03$                | $1700 \pm 100$                 |                                |                        |                        |                |
| 300 K | Dark      | CMR                            |                                | $1.40 \pm 0.05$                | $0.26 \pm 0.03$                | $1100 \pm 100$         | $2900 \pm 200$         |                |
|       |           | Hall                           | $1.30 \pm 0.03$                | $1900 \pm 100$                 |                                |                        |                        |                |

after short illumination pulses at either 5 or 77 K. In Fig. 5 we show the temperature dependence of  $n_{\text{Hall}}$  and  $\mu_{\text{Hall}}$  in the range from 5 to 300 K, measured in the dark and after illumination at 5 K.

We find that the Hall electron density,  $n_{\text{Hall}}$ , does not strongly depend on the temperature or the illumination conditions. The Hall mobility,  $\mu_{\text{Hall}}$ , shows a small increase when we increase the temperature above 80 K, but remains constant below 80 K. This temperature independence of the Hall mobility below 80 K is mainly due to the fact that we have a highly degenerate electron gas in which ionized impurity scattering is the main scattering mechanism.<sup>8</sup> In  $\delta$ -doped layers the mobility is considerably lower than in modulation doped GaAs/Al $_x$ Ga $_{1-x}$ As heterostructures, where ionized donors are separated from free electrons. Due to the very strong ionized impurity scattering, phonon scattering is not important in the whole temperature range. In the dark,  $\mu_{\text{Hall}}$  increases with temperatures above 80 K. We will later show that this is due to the population of the second subband, which has a higher mobility. After illumination at 5 K, the Hall mobility increases by about a factor of three. This mobility enhancement factor remains constant up to temperatures of about 80 K and it decreases at higher temperatures. At about 200 K the Hall mobility falls back to the dark value. Thus, persistent photoconductivity (PPC) is weakened above 80 K and above 200 K it disappears.

It is difficult to draw quantitative conclusions from these Hall measurements. This is due to the fact that in  $\delta$ -doped samples more than one subband is normally populated. The Hall density and Hall mobility, in such a case, depend on the strength of the magnetic field, the population of each subband, and the mobility in each subband.<sup>9</sup>

### C. Classical magnetoresistance measurements

In the case that multiple subbands are populated we can determine the carrier mobility and population in each individual subband from an analysis of the classical magnetore-

sistance measurements. Classical means that no quantum effects from the magnetic field should influence  $\sigma_{xx}(B)$  and  $\sigma_{xy}(B)$ , i.e., that no Schubnikov–de Haas oscillations or quantum Hall plateaus should be observed. In this classical regime the magnetoconductivity tensor elements are

$$\sigma_{xx}(B) = \sum_i \frac{qn_i\mu_i}{1 + (\mu_i B)^2} \quad \text{and} \quad \sigma_{xy}(B) = \sum_i \frac{qn_i\mu_i^2 B}{1 + (\mu_i B)^2}, \quad (1)$$

where  $\sigma_{xx}(B)$  is the longitudinal magnetoconductivity,  $\sigma_{xy}(B)$  the transversal magnetoconductivity or Hall conductivity,  $n_i$  the subband population,  $\mu_i$  the subband mobility, and  $q$  the elementary charge. The resistivity tensor elements  $\rho_{xx}(B)$  and  $\rho_{xy}(B)$  can be obtained by inverting the conductivity tensor.<sup>9</sup>

By analyzing the magnetic-field dependence of the  $\rho_{xx}(B)$  and  $\rho_{xy}(B)$  measurements, we obtain the individual subband mobilities and subband densities. We have used the mobility spectrum analysis technique proposed by Beck and Anderson<sup>10</sup> to obtain these values from classical magnetoresistance measurements.

The results obtained from the magnetoresistance measurements in the magnetic-field range from 0–5 T are shown in Table I. The results obtained at 77 K show that in the dark only one subband is populated. If the temperature is raised to room temperature it is clear that two subbands are populated. These results prove that above 80 K the second subband becomes populated by thermal redistribution of the free carriers. After illumination we also find that the second subband is populated. The persistent enhancement of the total electron concentration is due to neutralization of the depletion charges in the depletion regions next to the  $\delta$  layers.<sup>11</sup> We find a somewhat higher PPC effect in this structure than in our normal  $\delta$  layers. This is due to the fact that in  $\delta$ -doped structures we normally do not include Al $_x$ Ga $_{1-x}$ As barriers, which have a very high background concentration of defects when grown at 480 °C.

The second subband has a higher mobility compared to the lowest subband. This mobility enhancement is mainly due to the smaller overlap of the electron wave function in the second subband with the ionized impurity distribution compared to the overlap of electron wave function of the lowest subband.<sup>3</sup> The mobility enhancement after illumination at 77 K is smaller than after illumination at 5 K. We also observe a smaller persistent increase of the total electron density. During illumination at 77 K we cannot neutralize the depletion charges as effectively as during illumination at 5 K.

#### D. Schubnikov–de Haas measurements

In order to strengthen the arguments discussed in the previous paragraph we also performed Schubnikov–de Haas (SdH) measurements at 5 K.<sup>12</sup> The results of the SdH analysis are also shown in Table I. We find, just as in the classical magnetoresistance measurements, that only one subband is populated in the dark. The SdH measurements also show that after illumination a second subband is populated. The electron densities obtained from the SdH measurements compare reasonably with the densities obtained from the classical magnetoresistance analysis. From the magnetic-field dependence of the amplitudes of the SdH oscillations we are able to determine the quantum mobility of the carriers in each individual subband.<sup>13</sup> The quantum mobility is proportional to the scattering lifetime of a carrier, i.e., the scattering probability is not weighed by a factor  $\cos \theta$ , with  $\theta$  the scattering angle, as in the case for the transport mobility.<sup>14</sup> Similar to the transport mobilities obtained from the classical magnetoresistance measurements, we find that the mobility in the second subband is about a factor 3 higher than the mobility in the lowest subband. Finally, we would like to remark that a SdH analysis is only possible at temperatures below 40 K. Above this temperature the amplitude of the oscillations is so weak that it is impossible to analyze it properly.

#### E. Discussion of the subband structure

In  $\delta$ -doped structures with a doping concentration of about  $3 \times 10^{12} \text{ cm}^{-2}$ , we expect to find two populated subbands before illumination.<sup>7</sup> In the present structures in the dark we only find one populated subband below 80 K. We think that this is due to the high density of  $p$ -type defects in the  $\text{Al}_x\text{Ga}_{1-x}\text{As}$  barrier layers. We have the following arguments to support this idea. (1) Although we doped the structure at about  $3 \times 10^{12} \text{ cm}^{-2}$ , we only have  $1.6 \times 10^{12} \text{ cm}^{-2}$  free electrons. Thus many electrons are lost to deep defects. (2) In normal  $\delta$ -doped structures we find a persistent enhancement of the electron density after an illumination of approximately  $0.3 \times 10^{12} \text{ cm}^{-2}$ . In the present structure we find an enhancement of  $0.8 \times 10^{12} \text{ cm}^{-2}$ . Apparently there are more depletion charges that can be neutralized in the present structure. (3) If electrons from the doping layer are transferred to the  $\text{Al}_x\text{Ga}_{1-x}\text{As}$  layer, an electric field will form due to the charge separation. This electric field will lead to a steeper potential well and consequently to a further separation of the lowest and second subband. This can lift the energy position of the second subband above the Fermi level. If we perform self-consistent calculations we find that only a single subband is populated when the background concentra-

tion in the  $\text{Al}_x\text{Ga}_{1-x}\text{As}$  layer is about  $5 \times 10^{17} \text{ cm}^{-3}$ . This defect density is in agreement with defect concentration measurements we performed in homogeneous  $\text{Al}_x\text{Ga}_{1-x}\text{As}$  layers grown at 480 °C.

#### F. Conclusions from the sample characterization

In conclusion we have shown that in the dark at temperatures below 80 K only the lowest subband is populated. The second subband becomes populated by thermal excitation above 80 K. After illumination the second subband is also persistently populated. The mobility in the second subband is about 3 times the value of the mobility in the lowest subband. The population and mobilities in each subband are almost independent of temperatures below 80 K. Above 80 K the PPC effect starts to disappear.

### III. NOISE MEASUREMENTS AND DISCUSSION

The voltage fluctuations were measured in a frequency range from 1 Hz to 40 kHz by the four-point method. Details of the configuration for the noise measurement were described elsewhere.<sup>15</sup> We carried out noise measurements in the dark and also several minutes after illumination. The noise levels are proportional to the square of the voltage, and the length of the sample, which shows that the sample can be considered as a homogeneous Ohmic resistor.

Normally, a spectrum of low-frequency noise consists of thermal noise and  $1/f$  noise; sometimes generation-recombination ( $g-r$ ) noise is found. The thermal noise is the fluctuation of the velocities of electrons, and its power density  $S_v$  is given by Eq. (2). The  $g-r$  noise stems from  $g-r$  centers, and its power density  $S_{g-r}$  is described by equation (3).  $1/f$  noise is a fluctuation of the conductance. The origin of  $1/f$  noise is unknown. The normalized  $1/f$  noise  $S_R$  for Ohmic samples can be expressed by Eq. (4)<sup>16</sup>

$$S_v = 4k_B T R, \quad (2)$$

$$\frac{S_{g-r}}{V^2} = C \cdot \frac{\tau}{1 + (2\pi f \tau)^2}, \quad (3)$$

$$\frac{S_R}{R^2} = \frac{S_\sigma}{\sigma^2} = \frac{S_v}{V^2} = \frac{\alpha}{fN}, \quad (4)$$

where  $k_B$  is Boltzmann's constant,  $T$  is the temperature,  $R$  is the resistance,  $V$  is the voltage,  $C$  is a constant,  $\tau$  is the characteristic time of the  $g-r$  process,  $f$  is the frequency,  $\sigma$  is the conductance,  $\alpha$  is the noise parameter, and  $N$  is the total number of carriers in the volume involved in the noise generation. Some typical measured spectra are given in Figs. 6 and 7.

After illumination, at temperatures below 100 K we observed exact  $1/f$  noise. When we illuminated the samples below 100 K, the resistance of the sample decreases. Several minutes after turning off the light, the resistance became stable. The photoexcited electrons were frozen mainly in subband 2, the remainder in subband 1. The relaxation time is so long that the sample is stable enough for noise measurements. The noise after illumination was then measured. The spectra showed  $1/f$  noise (see Fig. 6). When the tem-

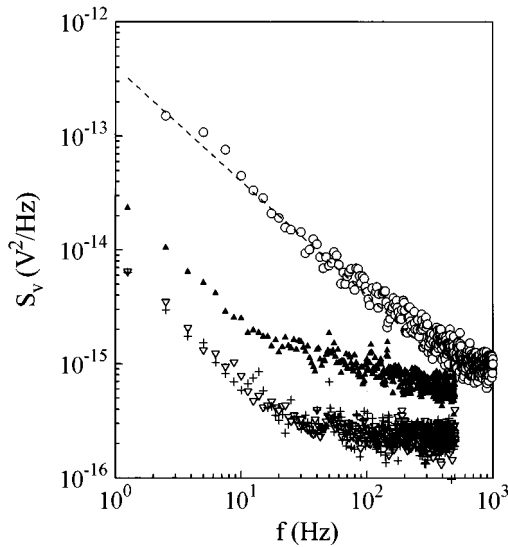


FIG. 6. Typical low-frequency noise spectra.  $\circ$ : in the dark at room temperature;  $\blacktriangle$ : in the dark at 77 K;  $+$ : several minutes after the illumination at 83 K.  $\nabla$ : several minutes after the illumination at 77 K. The dashed line  $\propto 1/f$  is for guiding the eye.

perature rises, the time dependence of PPC shows up. At temperatures above 100 K, the relaxation time became shorter than the time we needed for a noise measurement. Therefore, we could not measure the noise after illumination at higher temperatures.

In the dark, the noise was measured at temperatures from 77 to 300 K. Exact  $1/f$  noise spectra were again observed at temperatures below 100 K. We frequently observed  $g-r$  components in the spectra measured above 100 K due to deep levels in GaAs.<sup>17,18</sup> A detailed analysis of  $g-r$  noise is not included in this paper. However, the  $g-r$  noise was considered in the fitting procedure in order to determine accurately the  $1/f$  noise level (see Fig. 7).

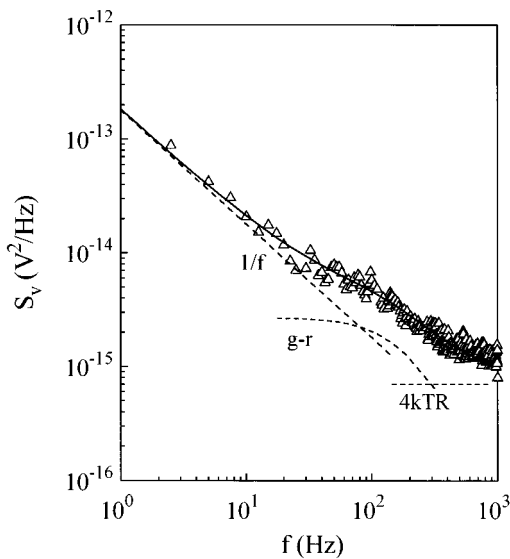


FIG. 7. A typical low-frequency noise spectrum with a  $g-r$  component.  $\triangle$ : measured in the dark at 191 K. The dashed lines represent the individual components of  $g-r$  noise,  $1/f$  noise, and thermal noise. The solid line represents the best fitting summation of the three noise components.

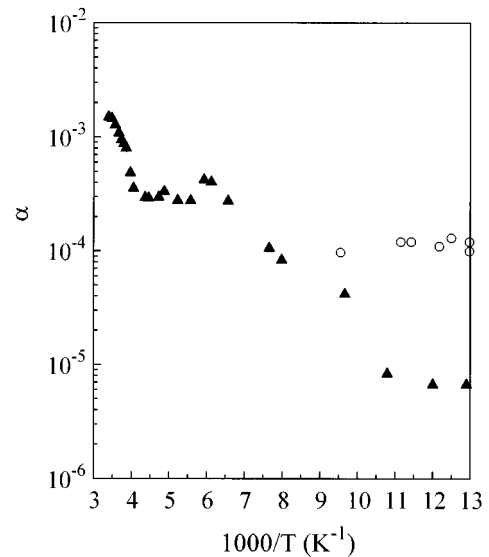


FIG. 8. Temperature dependence of the noise parameter  $\alpha$  determined by the Hall concentration.  $\circ$ : after illumination.  $\blacktriangle$ : in the dark.

In the following discussion of  $1/f$  noise, we shall characterize the  $1/f$  spectra by  $\alpha$  defined in Eq. (4), where  $N$  is obtained from  $N=l \times w \times n_{\text{Hall}}$ , with  $l$  and  $w$  the length and the width of the sample, and  $n_{\text{Hall}}$  the measured Hall concentration (Fig. 5).  $\alpha$  is an empirical parameter, expressing the relative strength of the  $1/f$  noise per electron.<sup>16</sup> The temperature dependence of  $\alpha$  is given in Fig. 8.  $\alpha$  in the dark increases quickly above 80 K. At temperatures below 80 K, the value of  $\alpha$  is much higher after illumination than in the dark. However, at 100 K, the value of  $\alpha$  after illumination and in the dark become comparable. It is clear that, in the dark, there is a transition from a low noise level to a high noise level. This transition starts to occur at 80 K and ends at about 100 K. As discussed in Sec. II, above 80 K, electrons are thermally redistributed so that the second level starts to be populated, this leads to the increase of the  $1/f$  noise. Above 100 K, the second subband contributes significantly to the  $1/f$  noise.

According to the above discussion, the noise increases very strongly when the second subband, with high mobility, is populated by either photoexcited electrons or thermally excited electrons. In other words, we observe a higher level of  $1/f$  noise, when the average mobility of electrons is higher. This encourages us to consider the model for  $1/f$  noise, where mobility fluctuations are only assumed in the lattice scattering.<sup>2,19</sup>

According to this model,  $S_{\mu_L} \neq 0$  and  $S_{\mu_{\text{imp}}} = 0$ . It is straightforward to derive from Matthiessen's rule

$$\alpha = \left( \frac{\mu}{\mu_L} \right)^2 \alpha_L, \quad (5)$$

where  $\alpha_L$  is a material constant,  $\mu$  the total mobility,  $\mu_L$  the mobility limited by the lattice scattering. Thus,  $\alpha$  is proportional to the square of the mobility. This model was described in detail in Refs. 2 and 19. The model works very well for the  $1/f$  noise in III-V compound materials.<sup>20,21</sup>

It could well be that the impurity scattering dominates the other scattering mechanisms. The average mobility  $\mu$  is then close to  $\mu_{\text{imp}}$ , the mobility due to impurity scattering. Nevertheless, only the lattice scattering generates  $1/f$  noise. The dominating impurity scattering then reduces the numerical value of  $\alpha$  according to Eq. (5).

In this  $\delta$ -doped sample, where two groups of electrons with different mobilities can contribute to the noise, we cannot simply put  $\alpha$  into Eq. (5) to determine  $\alpha_L$  for the  $\delta$ -doped layers. We have to determine the individual contribution by each group of electrons.

When the second subband gradually becomes populated, we should take into account that two types of carriers are present in the sample. We describe the  $1/f$  noise of the electrons in the two subbands system as noise from two parallel conduction mechanisms, i.e., from electrons in subband 1 and in subband 2. For the noise in the conductance we then write

$$\frac{S_\sigma}{\sigma^2} = \frac{S_{\sigma_1} + S_{\sigma_2}}{(\sigma_1 + \sigma_2)^2} = \frac{(n_1\mu_1)^2 \frac{\alpha_1}{n_1} + (n_2\mu_2)^2 \frac{\alpha_2}{n_2}}{(n_1\mu_1 + n_2\mu_2)^2} \frac{1}{fv}, \quad (6)$$

where  $n_i$  and  $\mu_i$  are the concentration and mobility of electrons in the  $i$ th subband, and  $v$  is the volume involved in the noise generation. Relation (4) has been used here for each type of electron.

Relation (7) directly follows from (4) and (6) without any further assumption or approximation,

$$\alpha = n_{\text{Hall}} \times \frac{n_1\mu_1^2\alpha_1 + n_2\mu_2^2\alpha_2}{(n_1\mu_1 + n_2\mu_2)^2}, \quad (7)$$

where

$$n_{\text{Hall}} = \frac{(n_1\mu_1 + n_2\mu_2)^2}{n_1\mu_1^2 + n_2\mu_2^2}, \quad (8)$$

hence,

$$\alpha = \frac{n_1\mu_1^2}{n_1\mu_1^2 + n_2\mu_2^2} \alpha_1 + \frac{n_2\mu_2^2}{n_1\mu_1^2 + n_2\mu_2^2} \alpha_2. \quad (9)$$

In the situation that two subbands are populated, we see that it is impossible to determine  $\alpha_1$  and  $\alpha_2$  by a single measurement. We need to prepare two situations with different distributions of the electrons over subbands 1 and 2 in order to obtain two independent equations with two unknown parameters  $\alpha_1$  and  $\alpha_2$ . We have seen that at 77 K we can prepare a situation with either one (in the dark) or two (after illumination) subbands populated. Thus, at 77 K we can find both  $\alpha_1$  and  $\alpha_2$ . Above 100 K there is no PPC effect and, therefore, we are not able to prepare two different situations. Hence we cannot determine  $\alpha_1$  and  $\alpha_2$  separately above 100 K.

Relation (9) will now be used for the analysis of the results that were obtained at 77 K, either in the dark or after illumination. Table I shows the numerical values to be used together with estimates of their errors. At 77 K, there is the advantage that the  $1/f$  noise from subband 1 in the dark can be separately measured due to the fact that the subband 2 is

not populated. The value of  $\alpha_1$  immediately follows from the dark situation since  $n_2=0$ . We obtain

$$\alpha_1 = 7 \times 10^{-6}. \quad (10)$$

We use  $\mu_{L1} = 2 \times 10^5 \text{ cm}^2/\text{V s}$  from Ref. 22. Relation (5) then yields

$$\alpha_{L1} = 0.3 \pm 0.1. \quad (11)$$

The analysis of the situation after illumination yields the value of  $\alpha_2$ . Assuming the same value in dark and after illumination for  $\alpha_1$ , we find that after illumination the term with  $\alpha_1$  in Eq. (9) is two orders of magnitude smaller than  $\alpha$ . Therefore we neglect the  $\alpha_1$  term in this case and find from Eq. (9)

$$\alpha_2 = 2 \times 10^{-4}. \quad (12)$$

The impurity scattering is different for the electrons in subband 1 and in subband 2, because of the different overlap of the electron wave functions with the impurity profile, but the lattice scattering is the same. Therefore we take  $\mu_{L2} = \mu_{L1}$  when applying Eq. (5)

$$\alpha_{L2} = 0.5 \pm 0.2. \quad (13)$$

We assume that this value, determined from the situation after illumination, is a constant, independent of the level of illumination. Comparing the results from (10)–(13) strongly supports our model with noise sources exclusively in the lattice scattering. Although  $\alpha_1$  and  $\alpha_2$  differ by a factor 30, they lead to  $\alpha_L$  values that are very close. In view of the inaccuracy we venture to conclude that they yield the same value:

$$\alpha_L = 0.4 \pm 0.2 \quad \text{at } 77 \text{ K}. \quad (14)$$

Comparing the value of  $\alpha_L$  in two dimensions (2D) with that in three dimensions (3D), we find that  $\alpha_L(2D) \approx 10^4 \times \alpha_L(3D)$ .<sup>23</sup> This high value may result (i) from the different number of the lattice modes involved, (ii) from the strongly disordered crystal lattice in the  $\delta$ -doped layer, where islands of Si have been observed. Strongly enhanced  $1/f$  noise has been found in disordered GaAs crystals.<sup>24–26</sup>

#### IV CONCLUSIONS

Our studies of the  $1/f$  noise in 2DEG structures have shown the following.

- (1) The electrons in a  $\delta$ -doped layer give a perfect  $1/f$  noise.
- (2)  $1/f$  noise in our samples is not due to any surface or interface effect.
- (3) The noise from the two lowest levels can be characterized by a single value  $\alpha_L$ , equal to 0.4.
- (4) The single value of  $\alpha_L$  supports the model in which fluctuations in the lattice scattering generate the  $1/f$  noise.

#### ACKNOWLEDGMENTS

The authors would like to thank Mr. W. C. van der Vleuten for the sample growth and Mr. P. A. M. Nouwens for the sample structuring.

- <sup>1</sup>F. N. Hooge, T. G. M. Kleinpenning, and L. K. J. Vandamme, *Rep. Prog. Phys.* **44**, 479 (1981).
- <sup>2</sup>F. N. Hooge, *IEEE Trans. Electron Devices* **41**, 1926 (1994).
- <sup>3</sup>G. Q. Hai, N. Studart, F. M. Peeters, P. M. Koenraad, and J. H. Wolter, *J. Appl. Phys.* **80**, 5809 (1996).
- <sup>4</sup>E. F. Schubert, J. E. Cunningham, and W. T. Tsang, *Solid State Commun.* **63**, 591 (1987).
- <sup>5</sup>K. Ploog, M. Hauser, and A. Fischer, *Appl. Phys. A* **45**, 233 (1988).
- <sup>6</sup>E. F. Schubert, J. E. Cunningham, and W. T. Tsang, *Appl. Phys. Lett.* **49**, 1729 (1986).
- <sup>7</sup>P. M. Koenraad, F. A. P. Blom, C. J. G. M. Langerak, M. R. Leys, J. A. A. J. Perenboom, J. Singleton, S. J. R. M. Spermon, W. C. van der Vleuten, A. P. J. Voncken, and J. H. Wolter, *Semicond. Sci. Technol.* **6**, 861 (1990).
- <sup>8</sup>K. Hirakawa and H. Sakaki, *Phys. Rev. B* **33**, 8291 (1986).
- <sup>9</sup>R. A. Smith, *Semiconductors* (Cambridge University Press, Cambridge, England, 1959), Chap. 5.
- <sup>10</sup>W. A. Beck and J. R. Anderson, *J. Appl. Phys.* **62**, 541 (1987).
- <sup>11</sup>L. X. He, K. P. Martin, and R. J. Higgins, *Phys. Rev. B* **36**, 6508 (1987).
- <sup>12</sup>P. M. Koenraad, in *Delta-Doping of Semiconductors*, edited by E. F. Schubert (Cambridge University Press, Cambridge, England 1996), Chap. 17.
- <sup>13</sup>P. M. Koenraad, B. F. A. van Hest, F. A. P. Blom, R. van Dalen, M. R. Leys, J. A. A. J. Perenboom, and J. H. Wolter, *Physica B* **177**, 485 (1992).
- <sup>14</sup>S. Das Sarma and F. Stern, *Phys. Rev. B* **32**, 8442 (1985).
- <sup>15</sup>X. Y. Chen, M. R. Leys, and F. W. Ragay, *Electron. Lett.* **30**, 600 (1994).
- <sup>16</sup>F. N. Hooge, *Phys. Lett.* **29A**, 139 (1969).
- <sup>17</sup>E. F. Schubert, *Doping in III-V Semiconductors* (Cambridge University Press, Cambridge, England, 1993), p. 59.
- <sup>18</sup>J. C. Bourgoin and H. J. von Bardeleben, and D. Stiévenard, *J. Appl. Phys.* **64**, R65 (1988).
- <sup>19</sup>F. N. Hooge and L. K. J. Vandamme, *Phys. Lett.* **A66**, 315 (1978).
- <sup>20</sup>L. Ren and M. R. Leys, *Physica. B* **172**, 319 (1991).
- <sup>21</sup>X. Y. Chen and M. R. Leys, *Solid-State Electron.* **39**, 1149 (1996).
- <sup>22</sup>G. E. Stillman, C. M. Wolfe, and J. O. Dimmock, *J. Phys. Chem. Solids* **31**, 1199 (1970).
- <sup>23</sup>F. N. Hooge and M. Tacano, *Physica B* **190**, 145 (1993).
- <sup>24</sup>M. E. Levinshtein and S. L. Rumyantsev, *Fiz. Tekh. Polyprovodn.* **29**, 1807 (1990) [*Sov. Phys. Semicond* **24**, 1125 (1990)].
- <sup>25</sup>X. Y. Chen and V. Aninkevicius, in *Proceedings of the 7th Vilnius Conference Fluctuation Phenomena in Physical Systems, Palanga, 1994*, edited by V. Palenskis (Vilnius University, Vilnius, 1994), p. 260.
- <sup>26</sup>L. Ren, *J. Appl. Phys.* **73**, 2180 (1993).